

A Novel Large-Vessel Arteritis in SARS-CoV-2-Related Multisystem Inflammatory Syndrome in Children (MIS-C)

- 1. Rida Salman, MD**
Baylor College of Medicine
Edward B. Singleton Department of Radiology, Texas Children's Hospital
- 2. Prakash Masand, MD**
Baylor College of Medicine
Edward B. Singleton Department of Radiology, Texas Children's Hospital
- 3. Thierry A.G.M. Huisman, MD**
Baylor College of Medicine
Edward B. Singleton Department of Radiology, Texas Children's Hospital
- 4. Maria Pereira, MD**
Baylor College of Medicine
Department of Pediatrics, Division of Rheumatology
- 5. Debra Lynn Kearney, MD**
Baylor College of Medicine
Department of Pathology & Immunology
- 6. R. Paul Guillerman, MD**
Baylor College of Medicine
Edward B. Singleton Department of Radiology, Texas Children's Hospital
- 7. Siddharth Jadhav, MD**
Baylor College of Medicine
Edward B. Singleton Department of Radiology, Texas Children's Hospital
Email address: spjadhav@texaschildrens.org
Address: Texas Children's Hospital, 6701 Fannin St #1400, Houston, TX 77030

The work originated from Texas Children's Hospital, 6701 Fannin St #1400, Houston, TX 77030.

Funding: N/A

Manuscript type: Case report

Keywords: SARS-Cov-2; MIS-C; Arteritis

Abstract

Multisystem inflammatory syndrome in children (MIS-C) is a newly defined condition associated with severe acute respiratory syndrome coronavirus 2 (SARS-CoV-2). The syndrome has been described as a "Kawasaki disease"-like illness and the spectrum of associated abnormalities, including vascular complications, remain to be fully defined. The novel findings of a large-vessel arteritis in this report will add to the understanding of this syndrome and its associated vascular complications.

Introduction

Multisystem inflammatory syndrome in children (MIS-C) associated with severe acute respiratory syndrome coronavirus 2 (SARS-CoV-2) has been described as a "Kawasaki disease"-like illness and the spectrum of associated abnormalities, including vascular complications, remain to be fully defined. Existing knowledge of the radiological findings in MIS-C is limited to a few case series [1,2]. A Morbidity and Mortality Weekly Report from the Centers for Disease Control and Prevention described the features of 570 cases (median age of 8 years with a range from 2 weeks to 20 years) of MIS-C in the United States between March and July 2020 [3]. Nearly 20% of these cases had coronary artery dilatation or aneurysm, but no other arterial involvement was described in this largest reported case series to date. In this report, we present a previously unreported large-vessel arteritis associated with this syndrome.

Case report

A thirteen-year-old girl was transferred from an outside institution to the emergency department of our quaternary children's hospital with a one-day history of generalized weakness, dyspnea, fever, vomiting and decreased oral intake. On presentation, she was tachycardic, hypertensive and febrile (Table 1).

She denied chest pain, cough, sore throat, abdominal pain, nausea, diarrhea, loss of smell or taste, loss of consciousness, epistaxis, ear or neck pain. She reported no COVID-19 contacts or other sick contacts. She is a non-smoker and reported no past medical or surgical history or allergies. She denied a family history of rheumatic disease.

On physical exam, the patient had normal conjunctiva, no skin rash, mild neck venous distention, tachycardia, cardiac gallop with III/VI regurgitant murmur at the apex, mild tachypnea with no respiratory distress, decreased lower extremities pulses when compared to the upper extremities, an abdominal bruit in the left upper quadrant, and hepatomegaly.

At the outside institution, a chest radiograph (CXR) reportedly showed vascular congestion with cardiomegaly. Labetalol was administered before she was transferred to our institution for hypertension. At our institution, an electrocardiogram showed sinus tachycardia with possible biventricular hypertrophy and diffuse T-wave flattening but no evidence of ischemia. A CXR showed small pleural effusions, cardiomegaly and an unusual retrocardiac paraspinal opacity (Fig 1a). Bedside transthoracic echocardiography (TTE) showed a moderately dilated left ventricle with global dysfunction, moderate mitral regurgitation, a normal aortic arch, normal coronary artery origins, and no pericardial effusion. The patient was diagnosed with acute heart failure. A single Lasix dose was given followed by milrinone and nitroprusside infusions upon transfer to the cardiovascular intensive care unit (CVICU). Upon arrival to CVICU, repeat TTE showed wall thickening of the descending thoracic and abdominal aorta and an irregular echogenic focus within the abdominal aorta suggestive of thrombus, for which a heparin infusion was initiated. CT angiography (Fig 1b-d) was then performed and showed extensive wall thickening and/or mural thrombus, luminal irregularity and multiple aneurysms of the descending thoracic and abdominal aorta, wall thickening and a saccular aneurysm of the proximal superior mesenteric artery, and proximal occlusion of the left main renal artery. An abdominal Doppler ultrasound study (Fig 2) showed similar aortic findings and no venous thrombosis. Upon admission, laboratory tests were pertinent for anemia, elevated inflammatory markers, elevated D-Dimer and troponin levels,

hyponatremia and hypocalcemia (Table 1). Reactive SARS CoV-2 IgG antibodies but no reactive SARS Cov-2 IgM antibodies were detected. SARS CoV-2 antigen PCR testing repeated on two consecutive days was negative. The above findings corroborated a diagnosis of multisystem inflammatory syndrome in children (MIS-C). Intravenous immune globulin, methylprednisolone, and broad-spectrum antibiotics including vancomycin and ceftriaxone were administered. Over the following days, no growth on blood culture was noted. In addition to the tabulated laboratory results (Table 1), anti-streptolysin O (ASO) and antinuclear antibody (ANA) antibody (including anti-double-stranded DNA and anti-SSA) testing were positive, while serology for HIV and syphilis was negative.

Cardiac magnetic resonance imaging (MRI) showed moderate dilatation of the right atrium and ventricle with mildly dilated pulmonary arteries, moderate to severe dilatation of the left atrium and ventricle, global ventricular hypokinesis and depressed systolic function with an ejection fraction of 31%, but no myocardial edema or delayed myocardial enhancement. MRI and MR angiography (MRA) of the brain was normal. MRA of the chest, abdomen and pelvis (Fig 3) showed extensive, non-enhancing wall thickening of the descending thoracic aorta and suprarenal abdominal aorta with a maximal thickness of 1.1 cm, consistent with wall edema and/or mural thrombus, with luminal irregularity and saccular aneurysms most notable of the suprarenal abdominal aorta where the aneurysm measured 5.2 x 3.5 cm. Severe narrowing of the left renal artery ostium was seen with absent opacification along its proximal course and distal reconstitution via collaterals with hypoperfusion of the left kidney. Mild hepatomegaly was also seen, but no venous thrombosis.

An infectious disease work-up revealed positive T-SPOT.TB and QuantiFERON interferon gamma release assay blood tests for tuberculosis, raising the possibility of tuberculous aortitis with mycotic aneurysms, and anti-tuberculous drugs were started. The patient underwent thoracoabdominal aortic aneurysm repair with a tetrafurcated graft, left renal artery stenting and splenectomy. Histopathologic inspection of the aorta revealed a noninfectious aortitis with features of large vessel

vasculitis (Fig 4). No granulomas or giant cells were noted, and the acid-fast stain for organisms was negative.

The immediate post-operative course was complicated by status epilepticus requiring multiple anti-epileptic drugs to achieve burst suppression. Brain MRI was pertinent for sequela of status epilepticus and post-ictal edema with interval improvement on a follow-up MRI. She was extubated to high flow nasal cannula, but developed severe cardiac systolic dysfunction requiring pressor support. In addition to MIS-C, the possibility of coronary abnormalities causing this systolic dysfunction was considered, but a coronary CTA showed no coronary artery stenosis or aneurysm.

The patient received anti-inflammatory and immunolytic therapy including intravenous methylprednisolone, two split doses of intravenous immunoglobulin (IVIG) and an interleukin-6 receptor antagonist (tocilizumab) with near normalization of inflammatory markers. After a 70-day hospital stay, the patient was discharged home in stable condition with further medical management.

Discussion

This teenage patient presented with fever and elevated inflammatory markers and manifested cardiac, gastrointestinal and hematologic organ involvement as well as a positive serology test for recent SARS-CoV-2 infection, meeting the CDC case definition of MIS-C [4]. The absence of mucocutaneous manifestations and coronary artery abnormalities on echocardiography, cMRI and chest MRA makes Kawasaki disease a less likely diagnosis. In addition, Kawasaki disease usually affects children at a younger age [5]. Other distinct features of MIS-C manifested in this case include the predominance of gastrointestinal symptoms and severely reduced cardiac function, as described in other case series [2,5,6]. Similar to prior reports [6,7], the elevation of procoagulant and inflammatory markers including prothrombin time, fibrinogen, D-dimer, AST, troponin, pro-BNP, ferritin, ESR and CRP were pertinent laboratory abnormalities in this patient.

Some of the imaging findings in this patient correspond to those previously reported in MIS-C [1,2] including central vascular congestion, pleural effusions, and hepatomegaly. However, to our knowledge, no cases of large-vessel arteritis have been previously reported in association with MIS-C. In a case series discussing the cardiac features, no evidence of vasculitis was noted in the three patients who underwent cross-sectional imaging [8].

To our knowledge, this is the first report of an MIS-C case manifesting with extensive aortic and branch artery abnormalities including aortitis, mural thrombus, saccular aneurysms and severe stenosis of the left renal artery ostium. The thrombotic findings are concordant with the hypercoagulable state described in adult patients with SARS-CoV-2 [9,10]. The patient exhibited ASO, ANA, anti-Ro/SSA and anti-thyroid antibodies that are not typically associated with large vessel vasculitis, and were possibly related to the immunologic response associated with MIS-C. The presence of hypertension, elevated ESR, and segmental descending thoracic and abdominal aortic luminal irregularity and aneurysms fulfill several of the Sharma minor criteria for the diagnosis of Takayasu arteritis and the European League Against Rheumatism/Pediatric Rheumatology International Trials Organization/Pediatric Rheumatology European Society classification criteria for childhood Takayasu arteritis [11]. However, it is unclear whether the patient's arteritis in this case was initiated or pre-existing and exacerbated by SARS-CoV-2 infection and MIS-C. The histopathology findings do not support an infectious, granulomatous, giant cell or non-inflammatory arteriopathy, and the positive interferon-gamma release assay blood testing for tuberculosis in this case may reflect latent rather than active disease. Also, tuberculous mycotic aneurysms typically occur in adults with rare exception [12,13]. Negative serologic testing for syphilis and blood cultures argue against other infectious causes of aortitis in this case.

There is increasing evidence of association between certain viral infections and vasculitis. Polyarteritis nodosa has been linked to hepatitis B virus infection with formation of multiple microaneurysms as well as corkscrewing of medium-sized arteries, most commonly the renal arteries, visible on catheter angiography or biopsy [14]. The vasculopathy associated with varicella-zoster

infection predominantly affects the brain, manifesting with variable patterns of arterial stenosis, arterial wall thickening and enhancement [15]. In addition, reports from Africa cite the occurrence of saccular aneurysms or pseudoaneurysms in HIV patients with a predilection for carotid and femoral vessels [16]. This documented linkage between certain viruses and vasculitis supports the possibility of an association between SARS-CoV-2 and development of vasculitis as seen in our case.

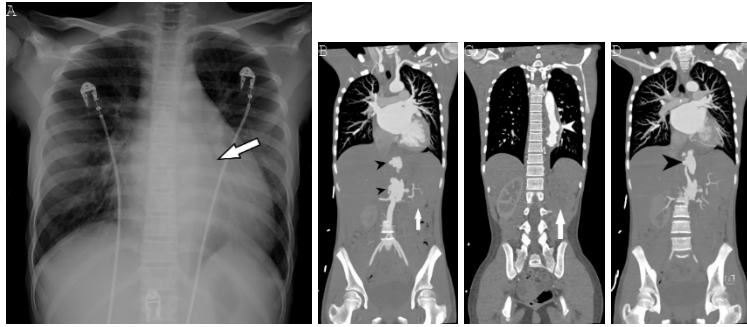
In conclusion, the phenotype of MIS-C associated with SARS-CoV-2 infection may include a large-vessel vasculitis that is characterized by wall inflammation, mural thrombus and aneurysms of the thoraco-abdominal aorta and branch arteries. Recognition of additional cases and further investigation of the clinical, laboratory and imaging features will provide further insight into MIS-C and the nature of its associated vascular complications.

References

1. Hameed S, Elbaaly H, Reid C, et al. Spectrum of imaging findings on chest radiographs, US, CT, and MRI images in multisystem inflammatory syndrome in children (MIS-C) associated with COVID-19. *Radiology* 2020. doi:10.1148/radiol.220202543. Published June 25, 2020. Accessed August 7, 2020.
2. Blondiaux E, Parisot P, Redheuil A, et al. Cardiac MRI of children with multisystem inflammatory syndrome (MIS-C) associated with COVID-19: case series. *Radiology* 2020. doi: 10.1148/radiol.2020202288. Published June 25, 2020. Accessed August 7, 2020.
3. Godfred-Cato S, Bryant B, Leung J, et al. COVID-19-Associated Multisystem Inflammatory Syndrome in Children - United States, March-July 2020. *MMWR Morb Mortal Wkly Rep.* 2020;69(32):1074-1080. Published 2020 Aug 14. doi:10.15585/mmwr.mm6932e2
4. Emergency preparedness and response: health alert network. Centers for Disease Control and Prevention website. <https://emergency.cdc.gov/han/2020/han00432.asp>. Published May 14, 2020. Accessed August 7, 2020.

5. Capone CA, Subramony A, Sweberg T, et al. Characteristics, cardiac involvement, and outcomes of multisystem inflammatory disease of childhood (MIS-C) associated with SARS-CoV-2 infection. *J Pediatr* 2020;224:141-145. doi:10.1016/j.jpeds.2020.06.044.
6. Whittaker E, Bamford A, Kenny J, et al. Clinical characteristics of 58 children with a pediatric inflammatory multisystem syndrome temporally associated with SARS-CoV-2. *JAMA*. 2020;324(3):259–269. doi:10.1001/jama.2020.10369.
7. Nakra NA, Blumberg DA, Herrera-Guerra A, Lakshminrusimha S. Multi-System Inflammatory syndrome in children (MIS-C) following SARS-CoV-2 infection: Review of clinical presentation, hypothetical pathogenesis, and proposed management. *Children (Basel)* 2020;7(7):69. doi: 10.3390/children7070069.
8. Ramcharan T, Nolan O, Lai CY, et al. Paediatric inflammatory multisystem syndrome: Temporally associated with SARS-CoV-2 (PIMS-TS): Cardiac features, management and short-term outcomes at a UK tertiary paediatric hospital. *Pediatr Cardiol*. 2020;1-11. doi:10.1007/s00246-020-02391-2. Published June 12, 2020. Accessed August 7, 2020.
9. Zhang Y, Xiao M, Zhang S, et al. Coagulopathy and antiphospholipid antibodies in patients with Covid-19. *N Engl J Med* 2020;382(17):e38. doi:10.1056/NEJMc2007575.
10. Emert R, Shah P, Zampella JG. COVID-19 and hypercoagulability in the outpatient setting. *Thromb Res* 2020;192:122-123. doi:10.1016/j.thromres.2020.05.031.
11. de Souza AWS, de Carvalho JF. Diagnostic and classification criteria of Takayasu arteritis. *J Autoimmun* 2014;48-49:79-83. doi: 10.106/j.jaut.2014.01.012.
12. Long R, Guzman R, Greenberg H, Safneck J, Hershfield E. Tuberculous mycotic aneurysm of the aorta: review of published medical and surgical experience. *Chest* 1999;115(2):522-531. doi:10.1378/chest.115.2.522.
13. Cox SG, Naidoo NG, Wood RJ, Clark L, Kilborn T. Tuberculous iliac artery aneurysm in a pediatric patient. *J Vasc Surg* 2013;57(3):834-836. doi:10.1016/j.jvs.2012.08.114.

14. Sharlala H, Adebajo A. Virus-induced vasculitis. *Curr Rheumatol Rep.* 2008;10(6):449-452. doi:10.1007/s11926-008-0073-y
15. Cheng-Ching E, Jones S, Hui FK, et al. High-resolution MRI vessel wall imaging in varicella zoster virus vasculopathy. *J Neurol Sci.* 2015;351(1-2):168-173. doi:10.1016/j.jns.2015.02.017
16. Pillay B, Ramdial PK, Naidoo DP. HIV-associated large-vessel vasculopathy: a review of the current and emerging clinicopathological spectrum in vascular surgical practice. *Cardiovasc J Afr.* 2015;26(2):70-81. doi:10.5830/CVJA-2015-017



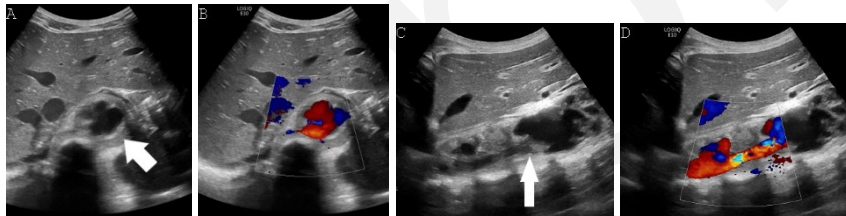
1a

1b

1c

1d

Fig.1: (A) Chest radiograph shows cardiomegaly and an abnormal left paraspinal density in the region of the descending thoracic aorta (arrow). (B, C and D) Coronal contrast-enhanced computed tomographic angiography images of the chest, abdomen and pelvis reveal a diffuse abnormal appearance of the descending thoracic aorta and suprarenal abdominal aorta with lumen irregularity, wall thickening and/or mural thrombus as well as multiple aneurysms (arrowheads). Lack of contrast opacification of the left renal artery and delayed enhancement of the left kidney (white arrow) secondary to renal artery stenosis or thrombosis.

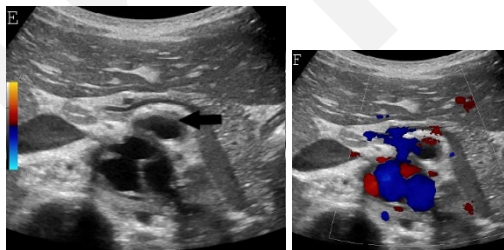


2a

2b

2c

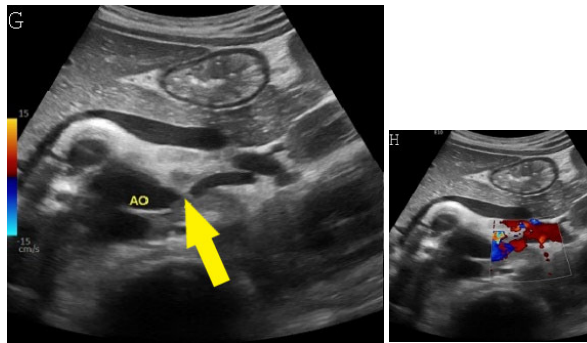
2d



2e

2f

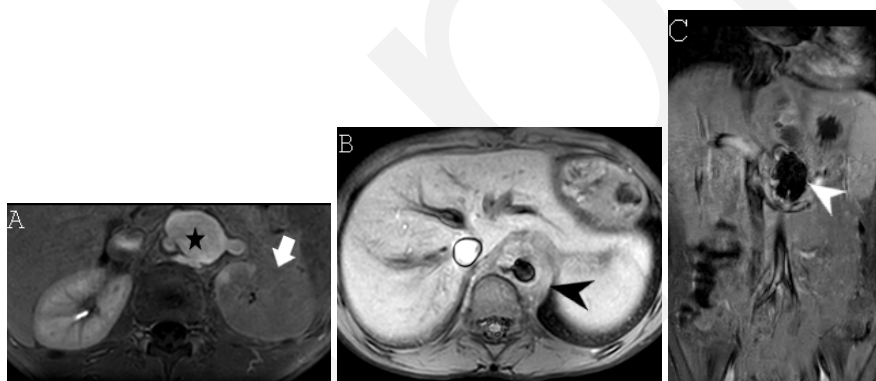
Fig. 2: (A,B,C,D) Transverse and sagittal gray-scale and color Doppler ultrasound images of the upper abdominal aorta (white arrow) and (E,F) transverse gray-scale and color Doppler ultrasound images of the superior mesenteric artery (black arrow) show wall thickening and/or mural thrombus, lumen irregularity, and multiple aneurysms.



2g

2h

(G,H) Transverse Gray-scale and color Doppler ultrasound images of the abdominal aorta and left renal artery (yellow arrow) show ostial narrowing of the left renal artery.



3a

3b

3c

Fig.3. (A) Axial triggered angiography non-contrast enhanced (TRANSE) MRI sequence shows suprarenal abdominal aortic aneurysm (star) and marked decreased signal intensity of the left renal parenchyma (arrow) compared to the right consistent with renal ischemia secondary to decreased perfusion. (B) Axial echo-planar image (EPI) MRI image and (C) Coronal EPI post-contrast MRI image

reveal non-enhancing aortic wall thickening (black arrow head) suggesting wall edema and/or mural thrombus. There is also undulating contour of the aortic lumen with saccular dilatation (white arrow head). (D) 3-D reconstructed image reveals the luminal irregularity and aneurysms of the thoraco-abdominal aorta.

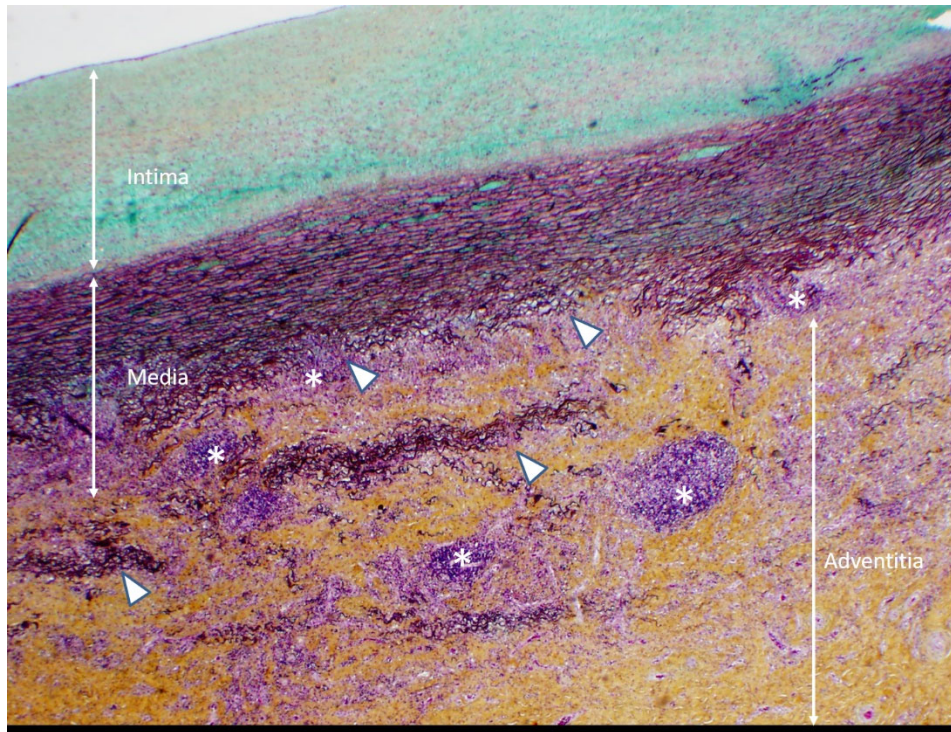


Fig. 4: Histopathological slide with Movat stain, 20x magnification. Noninfectious aortitis with patchy perivascular, adventitial and medial lymphocytic infiltrates (*). There is moderate thickening of the intima, variable medial thickening and disruption of elastic media (Δ) and marked, dense fibrotic thickening of the adventitia.

Table

Clinical and laboratory findings	Value	Normal Range
Pulse	128 beats/minute	60-100
Blood pressure	181/121 mmHg	110-131/64-83
Temperature	38.2 Celsius	36.3-37.6
Respiratory rate	38 breaths/minute	12-20
Weight	35 Kg	45.8 (average)
Body mass index (BMI)	12.7 Kg/m ²	18.5-24.9
Hemoglobin	9 g/dL	12-16
Mean Corpuscular Volume (MCV)	72.6 fL	76.9-90.6
White blood cell	7.47 * 10 ³ /uL	4.19-9.43
Ferritin	72 ng/mL	10-70
Troponin	0.23 ng/mL	<0.03
B-type natriuretic peptide (BNP)	1,602.4 pg/mL	<100
C-reactive protein (CRP)	5.1 mg/dL	<1
Procalcitonin	0.12 ng/mL	0.05-2
Lactate	1 mmol/L	0.2-1.7
Erythrocyte sedimentation rate (ESR)	101 mm/hour	0-20
Aspartate aminotransferase (AST)	36 U/L	10-30
Sodium	134 mmol/L	136-145
Potassium	4.4 mmol/L	3.5-5.5
Calcium	8.7 mg/dL	8.8-10.6
Creatinine	0.56 mg/dL	0.5-0.8

Albumin	3.6 g/dL	3.7-5
D-Dimer	2.1 microg/mL fibrinogen equivalent units	≤ 0.14
Fibrinogen	399 mg/dL	220-440
Platelet	280 * 10 ³ /uL	194-345
Prothrombin time (PT)	18.8 seconds	10.5-15.7
Partial thromboplastin time (PTT)	30 seconds	25.2-33.2
International normalized ratio (INR)	1.6	0.8-1.2
Thyroid stimulating hormone (TSH)	0.536 uIU/mL	0.7-4.1
Thyroxine (T4)	11.1 ug/dL	4.5-10
Lactate dehydrogenase (LDH)	579 U/L	380-640
Iron	51 ug/dL	55-150

Table 1: Clinical and laboratory findings obtained upon admission.